Progress in Oceanography 207 (2022) 102875

Contents lists available at ScienceDirect

Progress in Oceanography

journal homepage: www.elsevier.com/locate/pocean

Effects of climate change on the steric height and heat content in the Ballenas Channel, Gulf of California, Mexico (1939–2011)

David Serrano [a], Evlin Ramírez-Félix [b,*], Michel Hendrickx [c], Francisco Delgadillo-Hinojosa [d]

[a] Facultad de Ciencias del Mar, Universidad Autónoma de Sinaloa, Paseo Claussen s/n, C.P. 82000 Mazatlán, Sinaloa, Mexico
[b] Centro Regional de Investigación Acuícola y Pesquera en Mazatlán, Instituto Nacional de Pesca y Acuacultura, Sábalo-Cerritos s/n. Col. Estero El Yugo, 82112 Mazatlán, Sinaloa, Mexico
[c] Instituto de Ciencias del Mar y Limnología, Unidad Académica Mazatlán, Universidad Nacional Autónoma de México, Av. Joel Montes Camarena s/n, 82040 Mazatlán, Sinaloa, Mexico
[d] Instituto de Investigaciones Oceanológicas, Universidad Autónoma de Baja California, Carretera Transpeninsular Tijuana-Ensenada No. 3917, Fraccionamiento Playitas, Ensenada 22860, Baja California, Mexico

ARTICLE INFO

Keywords:
Steric height
Heat content
Sea level
Climate change
Gulf of California

ABSTRACT

The steric height (*StH*) and heat content (*HC*) are the integral variables most used as a measure of change of sea level at global scale. This study was carried out based on six data sets of average temperature and salinity profiles collected during the years 1939, 1962, 1974, 1984, 2003 and 2011 along the Ballenas Channel in the northern section of the Gulf of California. In order to eliminate high frequency thermal variability and evaluate its contribution in deep layers, *StH* and *HC* were calculated for the columns of 0–1000 m, 200–1000 m, 500–1000 m and 700–1000 m. We estimated *StH* rates of 1.0 ± 0.18 mm year^{-1}, 0.54 ± 0.14 mm year^{-1} and 0.30 ± 0.11 mm year^{-1} for the 200–1000 m, 500–1000 m and 700–1000 m columns, respectively. In particular, the contribution of the 700–1000 m column ranged from 15% in 1984 to 37% in 2011. We also found that the increase in *HC* in 72 years for the column of 200–1000 m was 1.6×10^9 Jm^{-2} representing an average net heating rate of 0.7 W m^{-2}. As a comparison, the average net heating rate in the Greenland Sea was 5.9 W m^{-2} for 13 years. This result may indicate that the marginal seas located below mid-latitudes could be less susceptible to the effects of climate change.

1. Introduction

Over the last century, global warming has been reflected regionally by a rise in sea level. It appears that steric height (*StH*) and heat content (*HC*) are the integral variables most used as a measure of change at oceanic level (Gaillard et al., 2016). *StH* results from the combined effect of temperature and salinity changes on seawater density, while *HC* expresses the temperature changes, both through the water column.

The sea level raise should be explained by the thermosteric expansion of the ocean water due to ocean warming, and ocean mass addition mainly due to continental ice and glacier melting (Bamber et al., 2007; Rignot et al., 2008; Chen et al., 2009; Jordà and Gomis, 2013). According to Bindoff et al. (2007), on a global scale the sea level has risen approximately at a rate of 1.7 to 1.8 mm year^{-1} between 1961 and 2003. In line with this work and using satellite observations, Ablain et al. (2009) reported values of 3.11 ± 0.6 mm year^{-1} in the 1993–2008 period; while Cazenave and Llovel (2010) reported a rate of 3.3 mm year^{-1} for almost the same period (1993–2007).

The seasonal variability of sea surface height can be explained by the upper ocean *StH*, suggesting that surface heat is basically stored above the seasonal thermocline (Kuhlbrodt and Gregory, 2012). However, the contribution to sea level rise can also be important in intermediate and deep layers of the ocean (Tsimplis and Rixen, 2002; Calvo et al., 2011). In particular, a rate of 1.1 mm year^{-1} has been reported as a global mean of the steric rise for the ocean below 700 m depth (Song and Colberg, 2011).

Relatively large increases in water temperature have been reported in marginal seas, due to the small volume to surface area ratio. Marginal seas tend to respond to global warming and changes in freshwater inputs much more strongly and rapidly than the open ocean (Schroeder et al.,

* Corresponding author.
E-mail addresses: davidse65@uas.edu.mx (D. Serrano), evlin.ramirez@inapesca.gob.mx (E. Ramírez-Félix), michel@ola.icmyl.unam.mx (M. Hendrickx), fdelgadillo@uabc.edu.mx (F. Delgadillo-Hinojosa).

https://doi.org/10.1016/j.pocean.2022.102875
Received 15 March 2022; Received in revised form 13 July 2022; Accepted 11 August 2022
Available online 17 August 2022
0079-6611/

2017). For example, the trend towards warming of sea surface or the deep layers of marginal seas from the Northwest Pacific Ocean (Seo et al., 2014) and the Arctic Ocean (Carvalho and Wang, 2020) are larger than the global and hemispheric averages.

On the other hand, thermal data at depths > 2000 m in the Mediterranean Sea showed a notable increase in the last 30 years (Vargas-Yáñez et al., 2017). Similarly, and although less noticeable, the same phenomenon was reported for the Central Greenland Sea between 200 and 2000 m depth over the 1981–1994 period (Bönisch et al. 1997).

We therefore consider that if there is evidence of climate change in the Gulf of California this should be reflected in the increase in both the *StH* and the *HC* recorded at Ballenas Channel. In a previous study, Beron-Vera and Ripa (2000) calculated the *HC* in the Gulf of California, including the Ballenas Channel, using temperature and salinity profiles from 1939 to 1985; however, to the best of our knowledge, there are not any studies on the *StH* variability and its relationship to climate change. Likewise, the mixing process reported in the Ballenas Channel (Simpson et al., 1994; López et al., 2008) play an important role in the warming of intermediate and deep waters.

This study is based on the calculation of *StH* and *HC*, using six average profiles of temperature and salinity up to a depth of 1000 m collected in the Ballenas Channel region. The profiles were recorded during the years 1939 (reported by Sverdrup et al., 1942), 1962, 1974 (reported by Gaxiola-Castro et al., 1978; Alvarez-Borrego et al., 1978), 1984, 2003 (Torres-Delgado et al., 2013) and 2011 (Hendrickx, 2012). The interval between the oldest and the most recent surveys was 72 years, with an interval between records > 7 years, allowing us to detect a trend of both *StH* and *HC* and provide evidence of climate change in the region.

This contribution is organized as follows. Section 2 briefly describes the study area and how the six average profiles of temperature and salinity were obtained. Also, in this section the algorithm used to obtain the *StH* and the *HC* is shown. The results describing the *StH* and *HC* variability and the TS diagram are presented in section 3. Finally, the discussion is presented in section 4 and the conclusions in section 5.

2. Methods

2.1. Study area and data collection

The study area is located in the Ballenas Channel, between Angel de la Guarda and San Lorenzo Islands (Midriff Islands Region) and the Baja California Peninsula (Fig. 1a). Compared to the rest of the Gulf of California (GC), the Ballenas Channel presents peculiar oceanographic characteristics such as the coldest and less saline surface water (Soto-Mardones et al., 1999) and it is considered an oceanographic province in itself (Lavín and Marinone, 2003). The Ballenas Channel has an irregular bathymetry and the presence of two sills that delimit the channel (Badan-Dangon et al., 1985; Paden et al., 1991). During spring tides, the height can reach 2.5 m in this area (CICESE, 2021) and tidal currents have been recorded in excess of 1 m s^{-1} (López et al., 2006). The high productivity and low surface temperature are associated with a mixing process caused by turbulence provoked by the interaction of strong tidal currents (López et al., 2008). Likewise, the flow over the sills generates internal waves producing high frequency fluctuations, contributing to the mixing of water column in Ballenas Channel (Simpson et al., 1994).

Several water masses have been reported in the Midriff islands: the Gulf of California Water, the Subsurface Subtropical Water, the Pacific Intermediate Water, and the Pacific Deep Water, with estimated proportional volumes of 39, 44, 16 and 1%, respectively (Hernández-Ayón et al., 2013). The maximum depth within the channel is ~ 1500 m, and the 16 oceanographic stations used during this study were located along the channel (Fig. 1b).

2.2. Temperature and salinity profiles and TS diagram

Year, date, and location of the sampling stations where temperature and salinity data were collected are shown in Table 1. The data from 1939 to 1985 were obtained from the NOAA World Ocean Data Base (https://www.ncei.noaa.gov/access/world-ocean-database-select/dbsearch.html). The more recent temperature and salinity profiles (1984–2011) were recorded using a CTD. In particular, during the Umbrales I, II and III campaigns (2002, 2003 and 2004, respectively) a SeaBird 911 Plus CTD was used whereas a SeaBird 19 was operated during the TALUD XIV campaign (2011). In the case of cruises carried out in 1939 and 1974, temperature and salinity were obtained with Nansen bottles, whereby we reconstructed the temperature and salinity profiles at every meter of depth using the Hermite polynomial interpolation. For the 1939 and 2011 campaigns, there was only one record in the area with a depth ≥ 1000 m.

The average profiles of temperature and salinity between 1962 and 2003 along with their respective standard error are shown in Figs. 2 and 3, respectively.

TS diagram was constructed with the purpose of identifying the

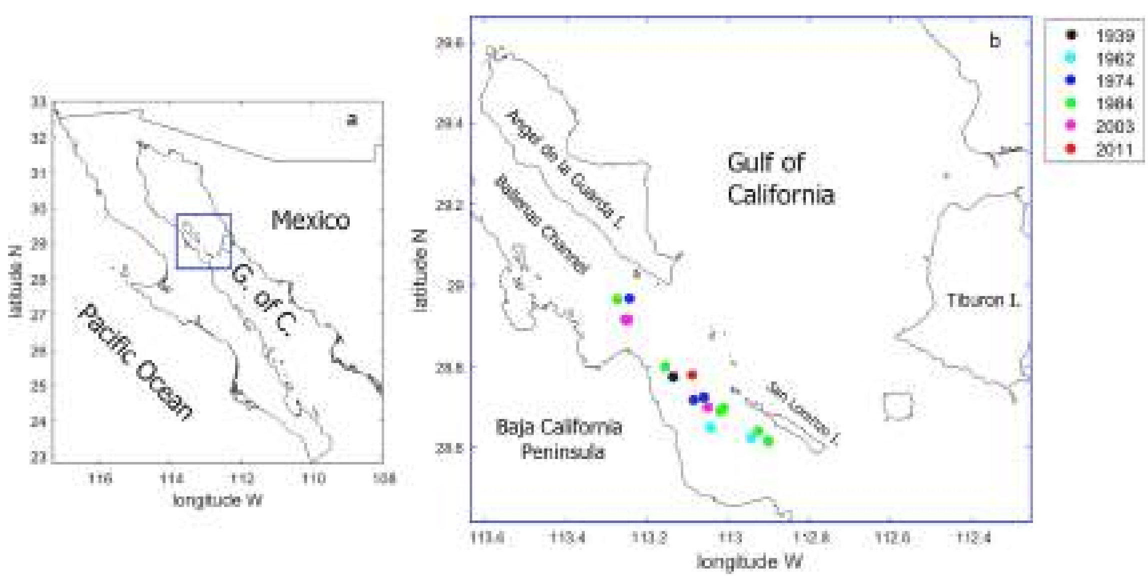

Fig. 1. Study area and sampling stations (colour-coded circles) in the northern Gulf of California. The blue rectangle in panel (a) is shown amplified in (b).

Table 1
Year, date, geographic position and source of temperature and salinity datasets used for the calculation of the average profiles.

Year	Date	Lat., Long.	Source
1939	03/19/1939	28.775 N, 113.133 W	NOAA
1962	11/03/196111/24/1963	28.650 N, 113.042 W28.625 N, 112.942 W	NOAA
1974	03/23/197310/14/197404/19/1974	28.718 N, 113.083 W28.967 N, 113.242 W28.725 N, 113.058 W	NOAA
1984	05/15/198405/26/198405/27/198411/23/198411/27/198403/17/1985	28.617 N, 112.900 W28.965 N, 113.272 W28.800 N, 113.153 W28.642 N, 112.925 W28.692 N, 113.017 W28.698 N, 113.010 W	NOAA
2003	03/18/200205/13/200309/05/2004	28.913 N, 113.249 W28.700 N, 113.048 W28.916 N, 113.252 W	Umbrales I, II, III
2011	04/12/2011	28.780 N, 113.087 W	TALUD XIV

water masses present during the distinct oceanographic cruises. In the same diagram, we added the average temperature and salinity for the 200–1000 m water column of the six periods, with the purpose of eliminating the seasonal variation of temperature and salinity that regularly occur in the upper 200 m (Beron-Vera and Ripa, 2000). In addition, an average profile of density for each period was calculated from the average temperature and salinity data in order to determine its trend over time. We also estimated the normalized Euclidean distance (ED) as a measure of similarity among TS curves (200–1000 m), with zero indicating complete similarity and 1 the maximum difference (Fig. 4).

2.3. Steric height and heat content

The steric height (*StH*, in mm) was calculated for the upper 1000 m water column using the thermodynamic equation of state (TEOS–10) following previous authors (Steele and Ermold, 2007; Dong and Zhou, 2013; Serrano and Valle-Levinson, 2021):

$$StH = \int_{h}^{H} \frac{\rho_{ref} - \rho_z}{\rho_{ref}} dz$$

where h is 0, 200, 500 or 700 m, H is 1000 m, ρ_z is the density at depth z and ρ_{ref} is a reference density. In this case, the density measured during the 1939′s cruise was taken as our reference density and corresponded with the values of 1028.68, 1029.16, 1029.84 and 1030.29 kg/m^3 for the 0–1000, 200–1000, 500–1000 and 700–1000 m layers, respectively. We also selected 1000 m as it was the common depth of θ and S_A of all cruises.

In addition, the heat content (*HC*, in J m^{-2}) of the water column was calculated following Cheng et al. (2010) and Serrano and Valle-Levinson (2021):

$$HC = \int_{h}^{H} C_{ps}\rho_z\left(T_z - T_{ref}\right)dz$$

where C_{ps} (~3992 J / kg °K) is the specific heat of seawater (IOC, 2010), ρ_z is water density, T_z is water temperature, T_{ref} is a reference temperature arbitrarily set to zero °C, h is 0, 200, 500 or 700 m and H is 1000 m.

Moreover, the *StH* was calculated for the 200–1000, 500–1000 and 700–1000 m layers. Reasons for this were: (1) to avoid intra-seasonal variability since the seasonal changes of θ and S_A are not relevant below 200 m depth in the Ballenas Channel (Millán-Núñez and Yentsch, 2000; Torres-Delgado et al., 2013); (2) to determine if any or some intermediate layers between 200 and 1000 m present an increase over time of *StH* and/or *HC*; (3) to evaluate the contribution of *StH* in the deep layers in order to compare it with the results of Song and Colberg (2011).

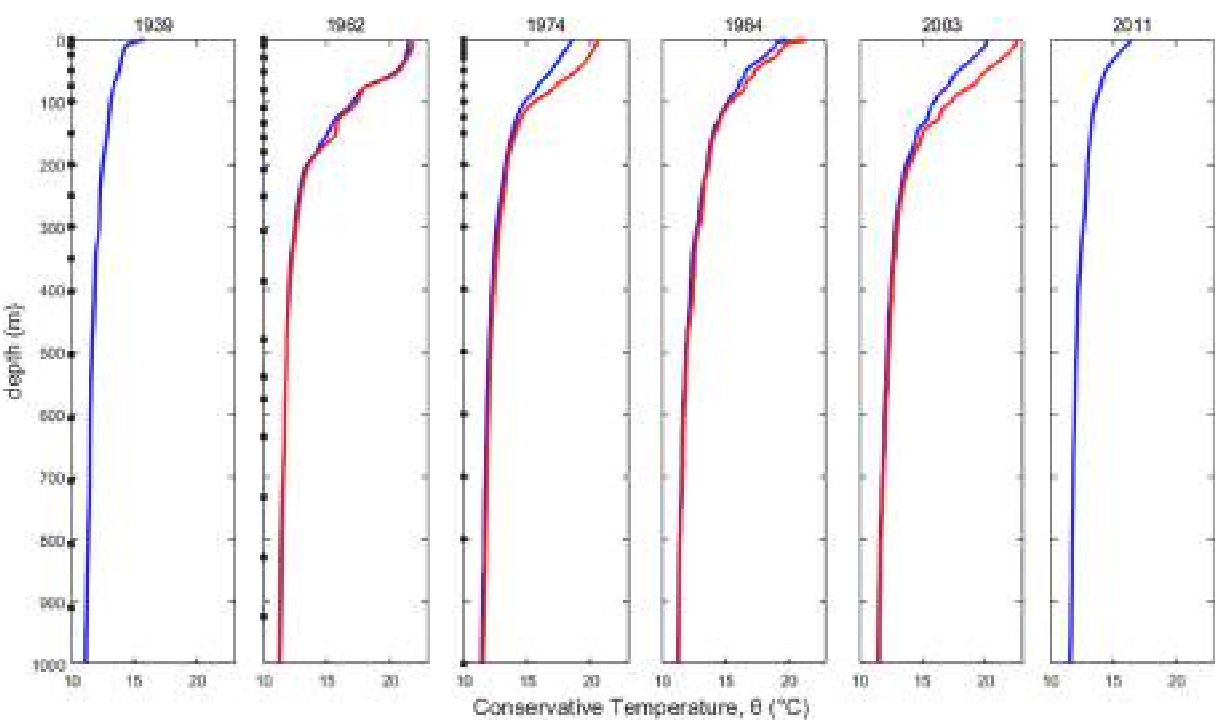

Fig. 2. Average temperature profiles (blue line) and its standard error (red line). The black squares on the y–axis indicate the depth at which the temperature was recorded with Nansen bottles during the cruises of 1939, 1962 and 1974.

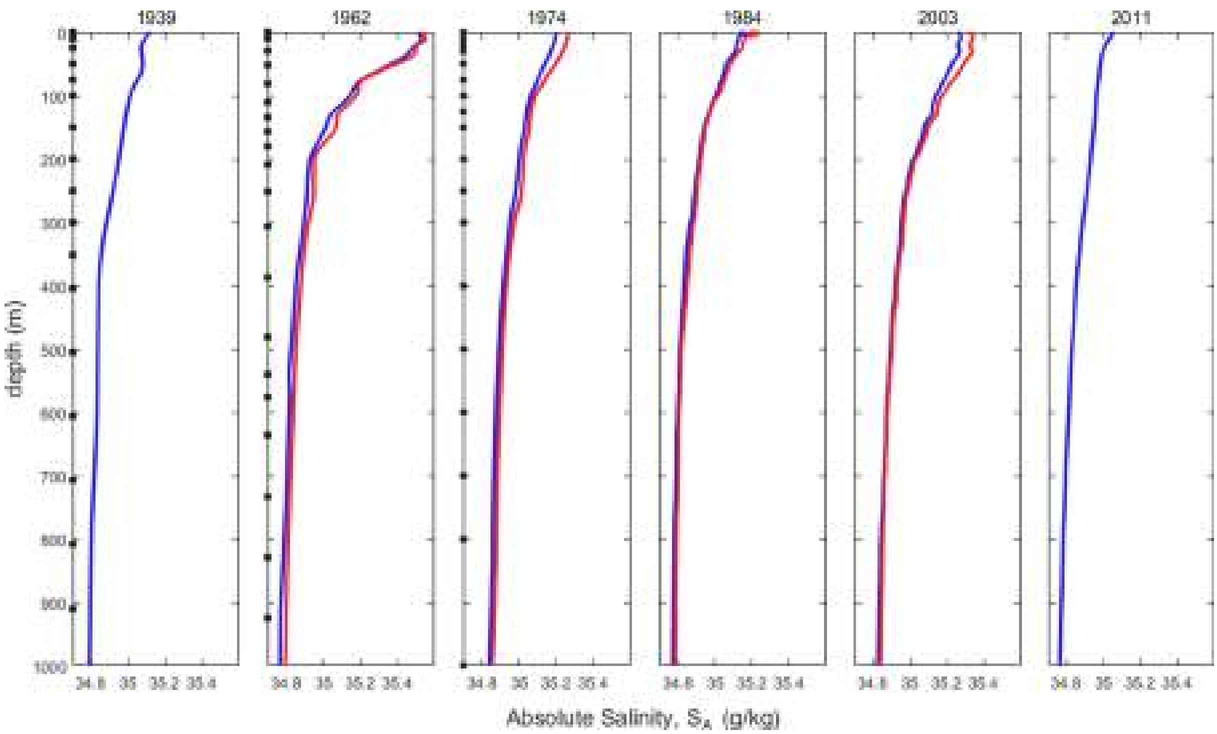

Fig. 3. The average absolute salinity profiles (blue line) and its standard error (red line). The black squares on the y–axis indicate the depth at which the temperature was recorded with Nansen bottles during the cruises of 1939, 1962 and 1974.

3. Results

3.1. θ and S_A profiles

The reconstruction of the temperature profiles for 1939, 1962, and 1974 campaigns as well as the average temperature profiles for years 1984, 2003 and 2011are shown in Fig. 2. In all temperature profiles, the greatest variation respect to depth occurred above 200 m. Below this depth, between 300 and 800 m, the temperature decreased steadily at an average rate of $\sim 2 \times 10^{-3}$ °C m^{-1}.

The maximum surface temperature (21.4 °C) was recorded in 1962 and the minimum (15.8 °C) was measured in 1939. Likewise, the maximum temperature at 1000 m was 11.56 °C in 2011 and the minimum was 11.14 °C in 1939. The maximum standard error (2.4 °C) was recorded on the surface in 2003 whereas the minimum standard error (0.12 °C) was observed at 1000 m in 1974.

The average salinity profiles and their standard error for the years 1962–2003, as well as the salinity profiles for the years 1939 and 2011, are shown in Fig. 3. The maximum surface salinity (35.51 g/kg) was recorded in 1962 whereas the minimum salinity (35.05 g/kg) was measured in 2011. Above 200 m, the greatest variation in salinity occurred in 1962 with 0.56 g/kg. The maximum standard error (0.07 g/kg) occurred at the surface in 1974. Below 200 m, all profiles showed that salinity decreased steadily at an average rate of 2.22×10^{-4} g/kg/m. The minimum salinity (34.76 g/kg) was recorded at 1000 m during the years 1962 and 2011.

3.2. TS curves

The six TS curves (Fig. 4) were clearly different. As expected, the greatest dissimilarity was found between the TS curves of 1939 and 2003 (ED = 1), and 1939 and 2011 (ED = 0.6). Besides, values less than or equal to 0.2 were estimated for consecutive TS curves: 1939–1962, ED = 0.2; 1962–1974, ED = 0.12; 1974–1984, ED = 0.09; 1984–2003, ED = 0.16 and 2003–2011, ED = 0.14.

The two main water masses detected throughout the study were the Gulf of California Water and the Subtropical Subsurface Water. The average temperature and salinity for the 200–1000 m layer (shown as open circles in Fig. 4a) were located at: 11.61 °C, 34.83 g/kg (1939); 11.79 °C, 34.82 g/kg (1962); 11.97 °C, 34.89 g/kg (1974); 11.91 °C, 34.81 g/kg (1984); 12.11 °C, 34.88 g/kg (2003); and 12.04 °C, 34.82 g/kg (2011). These results implied values of σ_t of 26.53, 26.49, 26.51, 26.46, 26.47 and 26.44 kg m^{-3} for the campaigns of 1939, 1962, 1974, 1984, 2003 and 2011, respectively (Fig. 4c). The slope of σ_t according to the fit was -1.1×10^{-3} kg m^{-3} year^{-1}.

3.3. Steric height (StH)

Taking the *StH* of 1939 as our reference value (zero mm), the temporal increase of *StH* for the 0–1000 m water column was neither clear nor constant between periods (1939–1962, 8.5 mm year^{-1}; 1974–1984, 6.1 mm year^{-1}; 1984–2003, 0.5 mm year^{-1}), even showing negative rates (1962–1974, −8.1 mm year^{-1}; and 2003–2011, −7.8 mm year^{-1}) (Fig. 5a). The poor temporal fit for the 0–1000 m water column may indicate high frequency steric height fluctuations in shallow layers.

After removing the layer of seasonal and high frequency influence (i.e., the upper 200 m), a remarkable temporal increase in steric height (Fig. 5b) is observed, presenting a positive trend in almost all intervals, with a maximum rate of 3.7 mm year^{-1} between 1974 and 1984 and a negative rate of −0.9 mm year^{-1} between 1962 and 1974. Thus, the average rate during the complete study period was 1.0 ± 0.2 mm year^{-1} (Fig. 5b).

For the 500–1000 m column, the positive trend was present in almost all intervals, except for a negative rate of −0.63 mm year^{-1} recorded in the 1962–1974 interval. The *StH* increase for this column was 0.54 ± 0.14 mm year^{-1}, which was half compared with the 200–1000 m column (Fig. 5c).

The increase in *StH* for the 700–1000 m column was lower compared to the upper columns (Fig. 5d), the average rate between the intervals was 0.5 mm year^{-1}, with a negative rate of −0.35 mm year^{-1} for the 1962–1974 interval. Overall, we calculated a slope of 0.30 ± 0.1 mm year^{-1}, indicating that in 72 years this layer presented an increase of 22

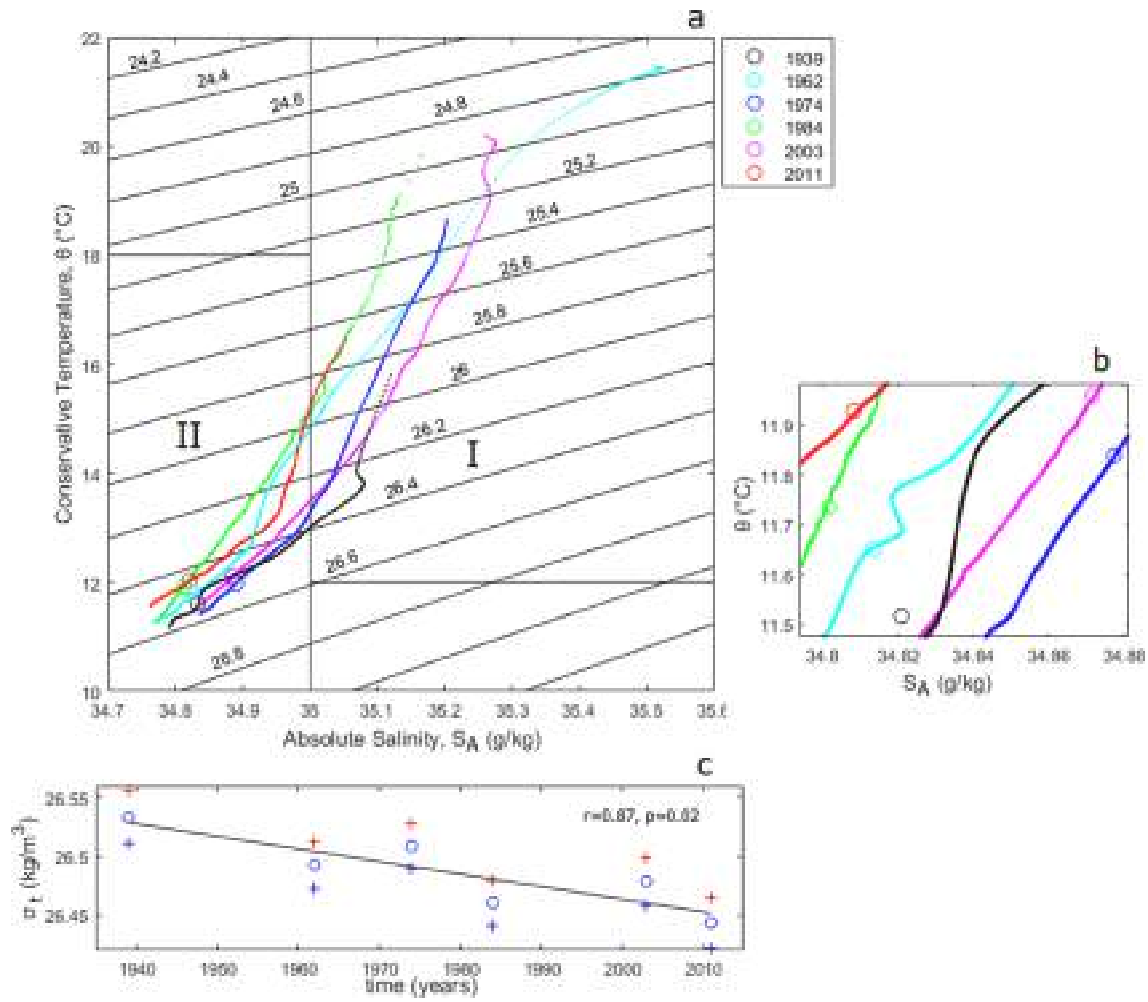

Fig. 4. (a) TS diagram. In panel (a) water masses correspond to the Gulf of California Water (I), and to the Subtropical Subsurface Water (II). (b) Zoom of (a). ○ Open circles in panels (a) and (b) represent the average temperatures and salinities for the 200–1000 m water column. (c) Time series of σ_t for the 200–1000 m water column. +symbols indicate the error limits associated with the linear fit.

mm.

Now if the steric height for the layer of 200–1000 m is taken as a reference (to eliminate the high frequency variations), the contribution to the increased steric height associated with the 700–1000 m layer for the years 1962, 1974, 1984, 2003 and 2011 were 20%, 24%, 15%, 28%, and 37%, respectively, revealing a clear upward trend over time.

3.4. Heat content

The heat content of the 0–1000 m water column did not show a clear increasing trend over time (Fig. 6a). There were two periods with negative rates in 1962–1974 (-0.96×10^8 J m^{-2} year^{-1}) and 2003–2011 (-2.5×10^8 J m^{-2} year^{-1}). In contrast, during the periods of 1939–1962 (1.7×10^8 J m^{-2} year^{-1}), 1974–1984 (0.3×10^8 J m^{-2} year^{-1}) and 1984–2003 (0.7×10^8 J m^{-2} year^{-1}) all rates were positive. Like the steric height, the poor fit for the 0–1000 m layer may be indicative of high frequency fluctuations of heat content in shallow layers.

Fig. 6b shows a clear increase of heat content for the 200–1000 m layer ($2.1 \times 10^7 \pm 4.1 \times 10^6$ J m^{-2} year^{-1}). Although there were two periods with negative rates (1974–1984 and 2003–2011) the positive rates predominated during the 1939–1962 (2.7×10^7 J m^{-2} year^{-1}, 1962–1974 (4.9×10^7 J m^{-2} year^{-1}) and 1984–2003 (3.6×10^7 J m^{-2} year^{-1}) periods.

The heat content trend over time in the 500–1000 layer was positive ($1.1 \times 10^7 \pm 2.6 \times 10^6$ J m^{-2} year^{-1}; Fig. 6c), with only one negative rate (-3.1×10^7 J m^{-2} year^{-1}) estimated for the 1974–1984 period. In general, the rate of heat content of this layer was slightly more than half that computed for the 200–1000 m water column.

Moreover, the heat content of the 700–1000 m layer also showed a positive trend ($6.3 \times 10^6 \pm 1.8 \times 10^6$ J m^{-2} year^{-1}; Fig. 6d), with a negative rate for the same period of 1974–1984. This rate was approximately half of that one calculated for the 500–1000 layer.

Finally, the average percentages of heat content of the 200–1000 m, 500–1000 m, and 700–1000 m layers, were 75.7%, 46.2%, and 27.5%, respectively, with the standard deviation for the three layers < 1.7%.

4. Discussion

The average temperature profiles recorded during the1939–2011 period in the central Gulf of California show notable differences above 200 m, which may be related to high frequency variability taking place in the surface and that, possibly, is masking or hiding the increased trend of surface temperature due to climate change. For example, according to the Oceanic Niño Index (ONI-NOAA), the maximum average surface temperature for the profile of 1962 could be due to a moderate El Niño with ONI of 1.4, recorded in November 1963. Likewise, in April 1974, a moderate La Niña with ONI of −1.0 was reported, and by April 2011, the ONI was −0.7, a weak La Niña. Some authors have pointed out that ENSO can dominate climate variability in tropical and subtropical

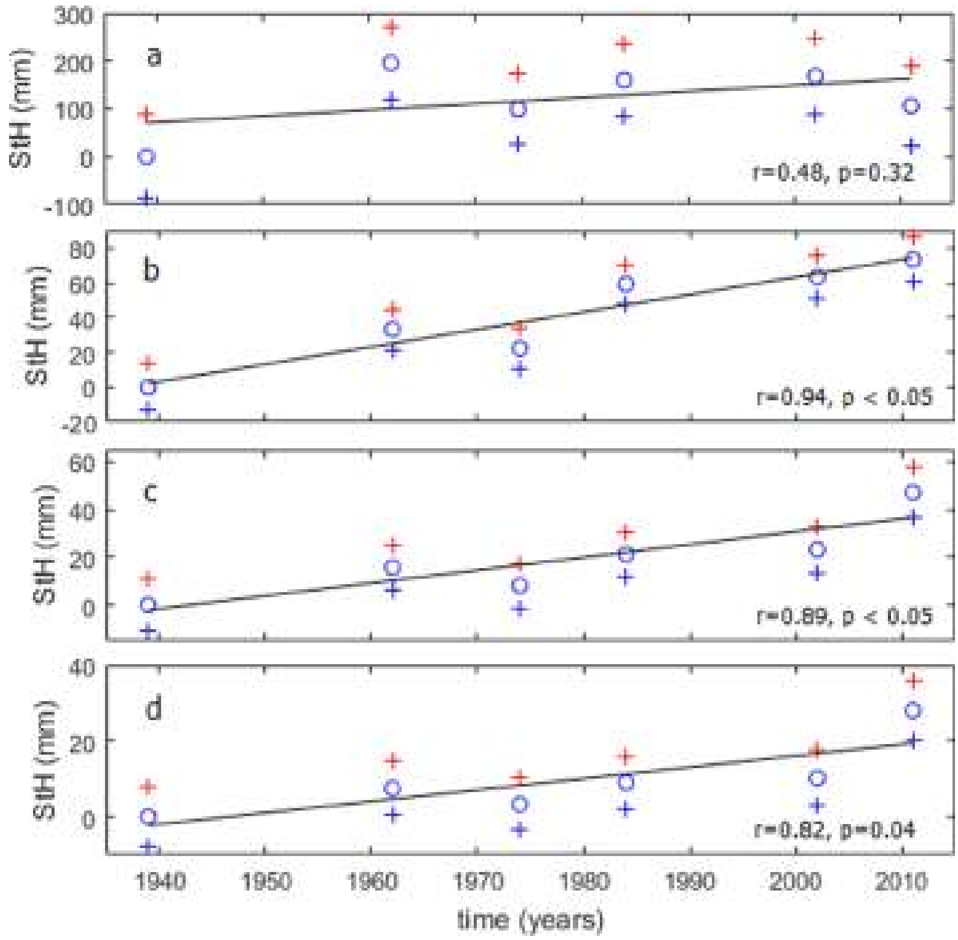

Fig. 5. Steric height (*StH*) calculated for the columns of (a) 0–1000 m, (b) 200–1000 m, (c) 500–1000 m and (d) 700–1000 m for 1962, 1974, 1984, 2003 and 2011. Calculations were performed putting $StH = 0$ for 1939 as the reference value. +symbols indicate the error limits associated with the linear fit.

regions and in some mid-latitude areas (Kumar and Hoerling, 1997). Supporting this hypothesis, Pérez-Arvizu et al. (2013) reported high unusual concentrations of chlorophyll-a in the Upper Gulf of California associated with the "El Niño-La Niña" transition in 2011. Likewise, between 200 and 1000 m, the θ profiles are similar and do not exceed 2.3 °C (2003 profile) difference. The poor stratification in this layer is the result of the mixing produced by the strong tidal currents taking place in this area (López et al., 2006).

On the other hand, we observed that σ_t for the 200–1000 m water column showed a negative temporal trend (slope of -1.1 x$10^{-3} \pm 0.3$ x10^{-3} kg m^{-3} year^{-1}; Fig. 4c), which was closely associated with the positive trend of average temperature (slope $= 6.3 \times 10^{-3} \pm 1.2 \times 10^{-3}$ °C year^{-1}, figure not shown) and that may be indicative of warming in intermediate waters as a consequence of the climate change. Our findings are consistent with those reported for other marginal seas. For example, Bönisch et al. (1997) described a remarkable decrease in density for intermediate waters (200–2000 m) in the Greenland Sea over the 1981–1994 period.

In the case of the 0–1000 m water column, the rate of *StH* was not constant during the five distinct intervals of time, with values ranging from 8 to 0.5 mm year^{-1} and negative rates in the 1962–1974 and 2003–2011 periods. The poor fit may indicate high frequency thermal variability in the upper layer in this section of the Gulf of California. Previous study had reported that *StH* values present an amplitude of 150 mm off the southeast coast of the Gulf of California (Serrano and Valle-Levinson, 2021), highlighting the important role played by the seasonal cycle controlling the amplitude of *StH* in this marginal sea.

Earlier works have used distinct methodologies and have reported on the sea level rising in the Gulf of California, thus it would be very illustrative to compare our results with these previous studies. For example, based on changes in tidal range, Páez-Osuna et al. (2016) considered the average trend of five tide stations with records spanning over more than 15 years and estimated that the increase in the average sea level rate within the Gulf of California was 2.5 ± 1.1 mm year^{-1}. In a similar way, Zavala-Hidalgo et al. (2010) compiled historical measurements (1951 to 1991) of tide gauges installed in the port of Guaymas (240 km SE of our study area). They concluded that the rate of sea level rise was 4.2 ± 1.7 mm year^{-1}. Although our estimates are lower than these previous reports for the Gulf of California, it seems significant to conclude that they are in the same order of magnitude. Furthermore, our results compare favorably with those rates measured in other marginal seas. For instance, in the Siberian Artic, the sea level increased at a rate of 1.85 mm year^{-1} over the 1954–1989 period (Proshutinsky et al., 2004). Likewise, in the Mediterranean Sea, before the 1960 s, the sea level increased at a rate of 1.2 mm year^{-1} (Tsimplis and Baker, 2000), whereas on the Norwegian coast a trend of 1.3–2.3 mm year^{-1} was estimated for the period of 1960–2010 by Richter et al. (2012).

The contribution of *StH* of the layers located below the seasonal thermocline is remarkable. For the 700–1000 m layer, the contribution of steric height is between 15 and 37%, with a tendency to increase over time. Song and Colberg (2011), based on a general circulation model, proposed that the layers below 700 m can contribute up to a third of the increase in sea level; our results indicate that they can contribute with ~ 40% in the Ballenas Channel region.

In this study, we observed that the heat content increases over time in the 200–1000 m, 500–1000 m, and 700–1000 m columns, with

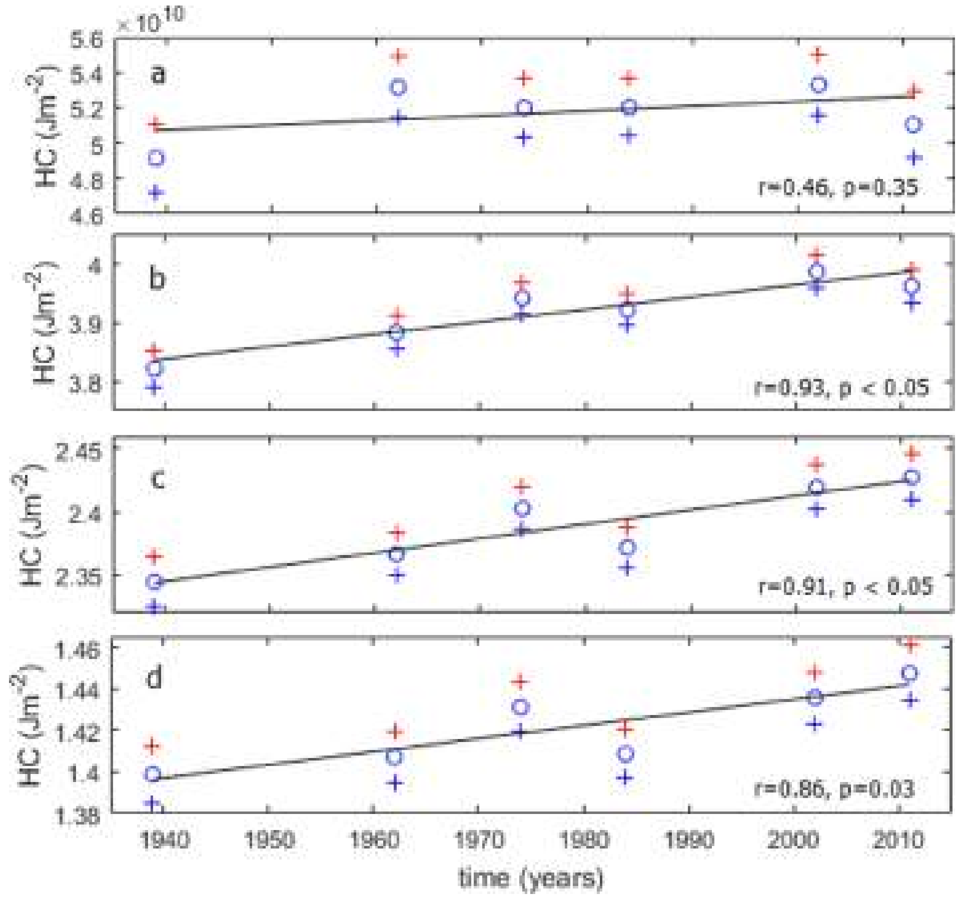

Fig. 6. Heat content (*HC*) for the columns of (a) 0–1000 m, (b) 200–1000 m, (c) 500–1000 m and (d) 700–1000 m for the years 1939, 1962, 1974, 1984, 2003 and 2011. +symbols indicate the error associated with the linear fit.

heating rates that decrease as depth increases and that, results in a vertically differentiated heating along the upper 1000 m of water column. Johnson et al. (2008) showed that several areas below 2000 m of the ocean began to experience warming since the 1990 s. Although our study was conducted in the 0–1000 m layer, our findings indicate that the heating rates decrease with depth likely due the existence of strong vertical mixing process produced by the intense tidal currents (López et al., 2008) and internal waves taking place in this area (Simpson et al., 1994).

The mixing process promotes the vertical transport of water from the surficial layers (depths < 200 m) downwards and, consequently, heat is transported from the surface to the deeper layers (see Fig. 2; López et al., 2008). A positive/negative surface heat flux will result in a positive/negative steric component (Jordà and Gomis, 2013). Alvarez-Borrego et al. (1978) showed that at a depth of 500 m inside the Ballenas Channel, the temperature was ~ 11.8 °C whereas outside the channel, at the same depth, the temperature was ~ 8 °C. These authors attributed this difference to the distinct mixing conditions existent between both sites.

A comparison that we consider interesting is the differentiation of global warming in two areas of the planet. In this study, the increase in heat content over a time-lapse of 72 years (200–1000 m layer) was 1.6×10^9 J m^{-2} (*HC* similar to that reported by Beron-Vera and Ripa, 2000, for the same year), which represents an average net heating rate of 0.7 W m^{-2}. On the other hand, Bönisch et al. (1997) reported for the Greenland Sea in the period 1981–1994 an increase in the heat content of 2.4×10^9 J m^{-2} in intermediate waters (200–2000 m), which represents an average net heating rate of 5.9 W m^{-2} for 13 years. Although the water column in the report by Bönisch et al. (1997) is 2.25 times higher than that obtained in the present work, the average net heating rate for the Greenland Sea was 8.4 times higher. A comparison of these observations may be an indication that the marginal seas located below mid-latitudes are less susceptible to the effects of climate change, but this does not mean that these effects are not important. One possible explanation for this statement is that the decrease in ice-covered areas at high latitudes has caused a decrease in albedo (Oppenheimer et al., 2019), and increased surface ocean heat absorption. We assume that the albedo at low latitudes has not changed significantly in recent years.

5. Conclusions

Based on six average profiles of temperature and salinity recorded in the Ballenas Channel during the 1939 –2011 period, we calculated that the steric height rates (mm year^{-1}) were statistically significant with a positive trend for the 200–1000 m, 500–1000 m and 700–1000 m layers. The heat content rates (J m^{-2} year^{-1}) for the same layers were positive with a clear tendency to decrease with depth. In contrast, when the whole water column (0–1000 m) was considered, the trend of both steric height and heat content of this layer was not clear due to high frequency thermal variability in the surface layer. Thus, our results of the temporal trend in heat content estimated for the Ballenas Channel may suggest that marginal seas located below mid-latitudes could be less susceptible to the effects of climate change when compared to seas located in higher latitudes.

This study underlines the crucial importance of using available historical data and highlights the necessity of carrying out systematic long-term monitoring of the water column, in order to quantify the trend of climate change in the region and the possible consequences on the water circulation and the existing natural communities. Our study shows the relevance of continuing to monitor the insular region of the Gulf of

California on a regular basis and, in general, pursuing the monitoring of the marginal seas which, as has been shown, are related with climate change.

Declaration of Competing Interest

The authors declare that they have no known competing financial interests or personal relationships that could have appeared to influence the work reported in this paper.

Acknowledgments

Ship time aboard the R/V "El Puma" was provided by the Coordinación de la Investigación Científica, UNAM (TALUD XIV). The authors thank all scientists, students and crewmembers who took an active part in the TALUD XIV cruise and, to the anonymous reviewers for their valuable suggestions, comments and time invested in improving the manuscript.

References

Ablain, M., Cazenave, A., Valladeau, G., Guinehut, S., 2009. A new assessment of the error budget of global mean sea level rate estimated by satellite altimetry over 1993–2008. Ocean. Sci. 5, 193–201. https://doi.org/10.5194/os-5-193-2009.

Alvarez-Borrego, S., Rivera, J., Gaxiola-Castro, G., Acosta-Ruíz, M.J., Schwartzlose, R.A., 1978. Nutrientes en el Golfo de California. Cienc. Mar. 5 (2), 53–71. https://doi.org/10.7773/cm.v5i2.322.

Badan-Dangon, A., Koblinsky, C.J., Baumgartner, T., 1985. Spring and summer in the Gulf of California: observations of surface thermal patterns. Oceanol. Acta. 8, 13–22.

Bamber, J.L., Alley, R.B., Joughim, I., 2007. Rapid response of modern day ice sheets to external forcing. Earth Planet Sc. Lett. 257, 1–13. https://doi.org/10.1016/j.epsl.2007.03.005.

Beron-Vera, J., Ripa, P., 2000. Threedimensional aspects of the seasonal heat balance in the Gulf of California. J. Geophys. Res. 105, 11441–11457. https://doi.org/10.1029/2000JC900038.

Bindoff, N.L., Willebrand, J., Artale, V., Cazenave, A., Gregory, J., Gulev, S., Hanawa, K., Le Quéré, C., Levitus, S., Nojiri, Y., Shum, C.K., Talley, L.D., Unnikrishnan, A., 2007. Observations: Oceanic Climate Change and Sea Level. In: Solomon, S., Qin, D., Manning, M., Chen, Z., Marquis, M., Averyt, K.B., Tignor, M., Miller, H.L. (Eds.), Climate Change 2007: The Physical Science Basis. Contribution of Working Group I to the Fourth Assessment Report of the Intergovernmental Panel on Climate Change. Cambridge University Press, Cambridge, United Kingdom and New York, NY, USA, pp. 385–432.

Bönisch, G., Blindheim, J., Bullister, J.L., Schlosser, P., Wallace, D.W.R., 1997. Long-term trends of temperature, salinity, density, and transient tracers in the central Greenland Sea. J. Geophys. Res. 102, 18553–18571. https://doi.org/10.1029/97JC00740.

Calvo, E., Simó, R., Coma, R., Ribes, M., Pascual, J., Sabatés, A., Gili, J.M., Pelejero, C., 2011. Effects of climate change on Mediterranean marine ecosystems: the case of the Catalan Sea. Clim. Res. 50 (1), 1–29. https://doi.org/10.3354/cr01040.

Carvalho, K., Wang, S., 2020. Sea surface temperature variability in the Arctic Ocean and its marginal seas in a changing climate: Patterns and mechanisms. Glob. Planet. Chang. 193, 103265 https://doi.org/10.1016/j.gloplacha.2020.103265.

Cazenave, A., Llovel, W., 2010. Contemporary sea level rise. Annu. Rev. Mar. Sci. 2, 145–173. https://doi.org/10.1146/annurev-marine-120308-081105.

Chen, J.L., Wilson, C.R., Blankenship, D.D., Tapley, B.D., 2009. Accelerated Antarctic ice loss from satellite gravity measurements. Nat. Geosci. 2, 859–862. https://doi.org/10.1038/NGEO694.

Cheng, P., Valle-Levinson, A., Winant, C.D., Ponte, A.L.S., Gutierrez de Velasco, G., Winters, K.B., 2010. Upwelling-enhanced seasonal stratification in a semiarid bay. Cont. Shelf Res. 30, 1241–1249. https://doi.org/10.1016/j.csr.2010.03.015.

(CICESE, 2021) http://predmar.cicese.mx/calmen/pdf/bla/bla2110.pdf.

Dong, L., Zhou, T.J., 2013. Steric sea level change in twentieth century historical climate simulation and IPCC-RCP8.5 scenario projection: a comparison of two versions of the FGOALS model. Adv. Atmos. Sci. 30 (3), 841–854. https://doi.org/10.1007/s00376-012-2224-3.

Gaillard, F., Reynaud, T., Thierry, V., Kolodziejczyk, N., von Schuckmann, K., 2016. In-situ based reanalysis of the global ocean temperature and salinity with ISAS: Variability of the heat content and steric height. J. Clim. 29, 1305–1323. https://doi.org/10.1175/JCLI-D-15-0028.1.

Gaxiola-Castro, G., Alvarez-Borrego, S., Schwartloze, R.A., 1978. El sistema de bióxido de carbono en el Golfo de California. Cienc. Mar. 5 (2), 25–40. https://doi.org/10.7773/cm.v5i2.324.

Hendrickx, M.E., 2012. Distribution and abundance of the pelagic processid, *Processa pippinae* Wicksten & Méndez, 1985 (Crustacea, Decapoda, Caridea, Processidae), collected during the TALUD XIV cruise in the Gulf of California, Mexico, and description of a new genus. Crustaceana 85 (4–5), 463–472. https://doi.org/10.1163/156854012X623773.

Hernández-Ayón, J.M., Chapa-Balcorta, C., Delgadillo-Hinojosa, F., Camacho-Ibar, V.F., Huerta-Díaz, M.A., Santamaría-del-Angel, E., Galindo-Bect, M.S., Segovia-Zavala, J. A., 2013. Dynamics of dissolved inorganic carbon in the Midriff Islands region of the Gulf of California: Influence of water masses. Cienc. Mar. 29, 183–201. https://doi.org/10.7773/cm.v39i2.2243.

IOC, 2010. The international thermodynamic equation of seawater – 2010: calculation and use of thermodynamic properties. Intergov. Oceanogr. Comm Manual and Guides 56, 1–207. https://doi.org/10.25607/OBP-1338.

Johnson, G.C., Purkey, S.G., Bullister, J.L., 2008. Warming and freshening in the abyssal southeast Indian Ocean. J. Clim. 21, 5351–5363. https://doi.org/10.1175/2008JCLI2384.1.

Jordà, G., Gomis, D., 2013. On the interpretation of the steric and mass components of sea level variability: the case of the Mediterranean basin. J. Geophys. Res. Oceans 118, 953–963. https://doi.org/10.1002/jgrc.20060.

Kuhlbrodt, T., Gregory, J., 2012. Ocean heat uptake and its consequences for the magnitude of sea level rise and climate change. Geophys. Res. Lett. 39 (L18608), 1–6. https://doi.org/10.1029/2012GL052952.

Kumar, A., Hoerling, M.P., 1997. Interpretation and implications of the observed inter-El Nino variability. J. Clim. 10, 83–91. https://doi.org/10.1175/1520-0442(1997)010<0083:IAIOTO>2.0.CO;2.

Lavín, M.F., Marinone, S.G., 2003. An overview of the physical oceanography of the Gulf of California. In: Velasco, O.U., Sheinbaum, J., Ochoa, J. (Eds.), Nonlinear Processes in Geophysical Fluid Dynamics. Springer, New York, pp. 173–204. https://doi.org/10.1007/978-94-010-0074-1_11.

López, M., Candela, J., Argote, M.L., 2006. Why does the Ballenas Channel have the coldest SST in the Gulf of California? Geophy. Res. Lett. 33 (L11603), 1–5. https://doi.org/10.1029/2006GL025908.

López, M., Candela, J., García, J., 2008. Two overflows in the Northern Gulf of California. J. Geophys. Res. 113, C08023. https://doi.org/10.1029/2007JC004575.

Millán-Núñez, E., Yentsch, C.M., 2000. El Canal de Ballenas, Baja California, como ambiente favorable para el desarrollo de fitoplancton. Hidrobiológica 10, 91–100.

(ONI-NOAA) Oceanic Niño Index. https://origin.cpc.ncep.noaa.gov/products/analysis_monitoring/ensostuff/ONI_v5.php.

Oppenheimer, M., Glavovic, B.C., Hinkel, J., van de Wal, R., Magnan, A.K., Abd-Elgawad, A., Cai, R., Cifuentes-Jara, M., DeConto, R.M., Ghosh, T., Hay, J., Isla, F., Marzeion, B., Meyssignac, B. and Sebesvari, Z., 2019: Sea Level Rise and Implications for Low-Lying Islands, Coasts and Communities. In: IPCC Special Report on the Ocean and Cryosphere in a Changing Climate [Pörtner, H.-O., Roberts, D.C., Masson-Delmotte, V., Zhai, P., Tignor, M., Poloczanska, E., Mintenbeck, K., Alegría, A., Nicolai, M., Okem, A., Petzold, J., Rama, B., Weyer N.M. (eds.)]. Cambridge University Press, Cambridge, UK and New York, NY, USA, pp. 321–445. https://doi.org/10.1017/9781009157964.006.

Paden, C.A., Abbott, M.R., Winant, C.D., 1991. Tidal and atmospheric forcing of the upper ocean in the Gulf of California. Part I. Sea surface temperature variability. J. Geophys Res. Oceans 96 (C10), 18337–18359. https://doi.org/10.1029/91JC01597.

Páez-Osuna, F., Sánchez-Cabeza, J.A., Ruiz-Fernández, A.C., Alonso-Rodríguez, R., Piñón-Gimate, A., Cardoso-Mohedano, J.G., FloresVerdugo, F.J., Carballo, J.L., Cisneros-Mata, M.A., Álvarez-Borrego, S., 2016. Environmental status of the Gulf of California: A review of responses to climate change and climate variability. Earth-Sci. Rev. 162, 253–268. https://doi.org/10.1016/j.earscirev.2016.09.015.

Pérez-Arvizu, E.M., Aragón-Noriega, E.A., Espinosa-Carreón, T.L., 2013. Variabilidad estacional de clorofila a y su respuesta a condiciones El Niño y La Niña en el Norte del Golfo de California. Rev. Biol. Mar. Oceanogr. 48, 131–141. https://doi.org/10.4067/S0718-19572013000100011.

Proshutinsky, A., Ashik, I.M., Dvorkin, E.N., Häkkinen, S., Krishfield, R.A., Peltier, W.R., 2004. Secular sea level change in the Russian sector of the Arctic Ocean. J. Geophys. Res. 109 (C3) https://doi.org/10.1029/2003JC002007.

Richter, K., Nilsen, J.E.Ø., Drange, H., 2012. Contributions to sea level variability along the Norwegian coast for 1960–2010. J. Geophys. Res. 117 (C5).

Rignot, E., Bamber, J.L., van den Broeke, M.R., Davis, C., Li, Y., van de Berg, W.J., van Meijgaard, E., 2008. Recent Antarctic ice mass loss from radar interferometry and regional climate modeling. Nat. Geosci. 1, 106–110. https://doi.org/10.1038/ngeo102.

Schroeder, K., Chiggiato, J., Josey, S.A., Borghini, M., Aracri, S., Sparnocchia, S., 2017. Rapid response to climate change in a marginal sea. Sci. Rep. 7, 4065. https://doi.org/10.1038/s41598-017-04455-5.

Seo, G.H., Cho, Y.K., Choi, B.J., Kim, K.Y., Kim, B., Tak, Y., 2014. Climate change projection in the northwest Pacific marginal seas through dynamic downscaling. J. Geophys. Res. Oceans 119 (6), 3497–3516. https://doi.org/10.1002/2013JC009646.

Serrano, D., Valle-Levinson, A., 2021. Effects of river discharge and the California Current on pycnocline depth at the eastern entrance to the Gulf of California. Cont. Shelf Res. 215, 104356 https://doi.org/10.1016/j.csr.2021.104356.

Simpson, J.H., Souza, A.J., Lavín, M.F., 1994: Tidal mixing in the Gulf of California, in Mixing and Transport in the Environment, edited by K.J. Beven, P.C. Chatwin, andJ. H. Millbank, pp. 169-182, John Wiley, New York.

Song, Y.T., Colberg, F., 2011. Deep ocean warming assessed from altimeters, Gravity Recovery and Climate Experiment, in situ measurements, and a non-Boussinesq ocean general circulation model. J. Geophys. Res. Oceans. 116, C02020. https://doi.org/10.1029/2010JC006601.

Soto-Mardones, L.A., Marinone, S.G., Parés-Sierra, A., 1999. Variabilidad espaciotemporal de la temperatura superficial del mar en el Golfo de California. Cienc. Mar. 25 (1), 1–30. https://doi.org/10.7773/cm.v25i1.658.

Steele, M., Ermold, W., 2007. Steric sea level change in the Northern Seas. J. Clim. 20, 403–417. https://doi.org/10.1175/JCLI4022.1.

Sverdrup, H.U., Johnson, M.W., Fleming, R.H., 1942. The Oceans. Prentice-Hall Inc, New York.

Torres-Delgado, E.V., Delgadillo-Hinojosa, F., Camacho-Ibar, V.F., Segovia-Zavala, J.A., Huerta-Díaz, M.A., Hernández-Ayón, J.M., Galindo-Bect, S., 2013. Wintertime enrichment of inorganic nutrients in the Ballenas Channel, Gulf of California. Cienc. Mar. 39, 47–64. https://doi.org/10.7773/cm.v39i2.2236.

Tsimplis, M.N., Baker, T.F., 2000. Sea level drop in the Mediterranean Sea: An indicator of deep water salinity and temperature changes? Geophys. Res. Lett. 27 (12), 1731–1734.

Tsimplis, M.N., Rixen, M., 2002. Sea level in the Mediterranean Sea: The contribution of temperature and salinity changes. Geophys. Res. Lett. 29 (23), 2136. https://doi.org/10.1029/2002GL015870.

Vargas-Yáñez, M., García-Martínez, M.C., Moya, F., Balbín, R., López-Jurado, J.L., Serra, M., Zunino, P., Pascual, J., Salat, J., 2017. Updating temperature and salinity mean values and trends in the Western Mediterranean: The RADMED project. Progr. Oceanogr. 157, 27–46. https://doi.org/10.1016/j.pocean.2017.09.004.

Zavala-Hidalgo, J., de Buen-Kalman, R., Romero-Centeno, R., Hernández-Maguey, F., In: A.V. Botello, S. Villanueva-Fragoso, J. Gutiérrez, y J.L. Rojas Galaviz (ed.), 2010. Tendencias del nivel de mar en las costas mexicanas. Vulnerabilidad de las zonas costeras mexicanas ante el cambio climático, 2nd. SEMARNAT-INE, UNAM-ICMyL, Universidad Autónoma de Campeche, México, pp. 249–268.